A MULTI-FREQUENCY APPROACH TO INCREASE THE NATIVE RESOLUTION OF ULTRASOUND IMAGES

François Varray[1], *Christian Cachard*[1], *Jan Kybic*[2], *Anthony Novell*[3], *Ayache Bouakaz*[3], *Olivier Basset*[1]

[1] Université de Lyon, CREATIS ; CNRS UMR5220 ; Inserm U1044 ; INSA-Lyon ; Université Lyon 1 ; Villeurbanne, France, name@creatis.univ-lyon1.fr
[2] Center for Machine Perseption, Department of Cybernetics, Czech Technical University, Prague
[3] UMR Inserm U930 CNRS ERL 3106, Tours, France

ABSTRACT

In ultrasound (US), a natural competition exists between the resolution of the image and the depth-of-field (DOF) into the medium, competition which is difficult to overcome with current US probe. Using large bandwidth transducer, such as cMUT, and the possibility to transmit several frequencies in one single transmission, we propose a multi-frequency scheme based on the frequency compounding (FC) technique to improve the native resolution of the US image and the DOF. In a first time, the different images at the different frequencies are created and a specific time-gain-compensation is used to compensate for the frequency attenuation. Then, the multi-frequency (MF) image is created in order to enhance the resolution and the SNR in the radio frequency domain. The resulting evaluations, through simulations and experiments, show a visible increase of the SNR and of the resolution. Moreover, the exploration depth is improved thanks to the attenuation compensation.

Index Terms— Multi resolution, ultrasound, cMUT, radio frequency image, frequency compounding

1. INTRODUCTION

In medical ultrasound (US) imaging, a natural competition exists between the image resolution and the depth-of-field (DOF). Indeed, the higher the frequency, the higher the resolution and the shorter the DOF [1]. In order to overcome this limitation, it is necessary to access for high frequency content to maintain a high resolution and low frequency information to go deeper into the tissue. The relative bandwidth of a piezoelectric transducer (PZT) is the difference between the two upper and lower frequencies at -6 dB divided by the peak frequency. With current PZT technologies, the bandwidth is generally limited in the range 60% to 100%, and does not allow the transmission of several distinct frequencies into the medium [2]. Capacitive micromachined ultrasound transducer (cMUT) offers many advantages compared to classical PZT such as the large frequency bandwidth. Indeed, the bandwidth of a cMUT in transmit mode is usually larger than 100% and theoretically infinite in receive mode [2]. Using such transducers, the range of frequencies that can be transmitted into the medium is much bigger than with the PZT.

In order to combine images of the same medium acquired with different frequencies, the classical frequency compounding (FC) technique is used [3]. Although it increases the signal-to-noise ratio (SNR), the FC also reduces the resolution of the US image but compensate the medium attenuation [4, 5]. In this paper, we proposed to use a large band transducer coupled with a multi-frequency approach in order to increase the resolution and the SNR of the US image. Using such bands, low and high frequencies are transmitted in the medium. A FC scheme is then used but coupled with a specific attenuation correction to create the final multi-frequency (MF) image. The compounding is made into the radio frequency domain in order to increase the resolution and not on B-mode imaging as in classical FC.

The paper is organized as follows. First, the mathematical background of the MF approach is presented. Then, the resulting images obtained in simulations and experiments with classical beamforming and MF image are presented. Finally, conclusions and discussions are drawn.

2. MATHEMATICAL BACKGROUND

2.1. Objectives

The FC consists in imaging the same medium with N different frequencies. The elementary log-compressed images are then summed in order to decrease the speckle noise and increase the signal-to-noise ratio (SNR) [6]:

$$I^{FC} = \sum_{i=1}^{N} I_i^{log} \tag{1}$$

where I_i^{log} is the i^{th} log-compressed image of the medium at the frequency f_i.

The idea of the proposed method consists in taking advantage of the broad frequency band of new transducers, such as

the cMUT, in order to transmit different frequencies in a single shot. Then, in receive mode, the recorded radio-frequency (RF) signal is decomposed into N sub-bands. Thanks to the large bandwidth of the transducer, it is possible to decompose the received signal into separated frequency components and to create an image taking advantage of the low frequencies for the penetration depth and on the high frequencies for the resolution.

2.2. Attenuation compensation

The use of separated frequencies in reception emphasizes the problem of the attenuation. Indeed, in biological media, the attenuation function is frequency dependent and high frequencies are attenuated faster during the propagation. In this way, before summing the elementary images, time gain compensation (TGC) is required to decrease the effect of the attenuation. A specific TGC_i has to be used on the i^{th} elementary image in order to correctly compensate for each frequency component. Using the notation $\hat{I}$ for the attenuation compensated images, the compensation is expressed as:

$$\hat{I}_i^{log} = I_i^{log} + TGC_i \tag{2}$$

Biological medium are usually considered with an attenuation dependent law expressed as [6]:

$$\alpha_i = \alpha_0 f_i^{\gamma} \tag{3}$$

where f_i is the frequency of the i^{th} elementary image (Hz), α_0 the attenuation constant (dB.m^{-1}.Hz$^{-\gamma}$), and γ the attenuation power law. Using such a formulation, the i^{th} TGC can be expressed at a depth z with:

$$TGC_i = \alpha_i z \tag{4}$$

The major drawback of the FC image is the resolution reduction which comes from the fact that the FC image is made after the log-compression step. Moreover, the phase and frequency information of the signal is lost during the transformation of the RF image into the log-compressed one. These two major issues are disadvantageous for the MF approach proposed in the paper. To create the final MF image, the elementary images must be kept as long as possible into the RF domain in order to take benefit of the phase and frequency content. The attenuation compensation is made on the RF data and the FC also. The envelope detection is performed only once on the final MF RF image. The elementary i^{th} attenuation compensated RF image, $\hat{I}_i^{RF}$, is expressed with the attenuation compensation as:

$$\hat{I}_i^{RF} = I_i^{RF} \times e^{\alpha_i z \ln(10)/20} \tag{5}$$

The final MF RF image, $\hat{I}^{MF}$, reconstructed with the N multi-frequency levels, is expressed as:

$$\hat{I}^{MF} = \sum_{i=1}^{N} \hat{I}_i^{RF} = \sum_{i=1}^{N} I_i^{RF} \times e^{\alpha_i z \ln(10)/20} \tag{6}$$

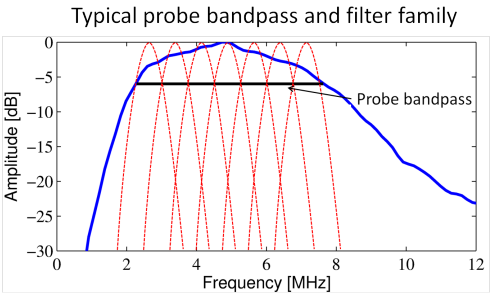

Fig. 1. Theoretical frequency spectrum of the probe used in simulation (blue solid line) and its bandwidth (black horizontal line). The spectrum is a modified version of a prototype cMUT array [7]. The red-dashed curves represent the filters used for the case N=7.

Using the final MF RF image, the envelope detection and the log-compression can be conducted in order to compare the obtained image to the initial image itself.

2.3. Filtering strategy

From the initial band-pass of the probe, different strategies of decomposition can be used. In this preliminary study, a simple decomposition into different frequency bands, using a 5^{th}-order Butterworth filter has been used. From the width of the initial band-pass, the N images are created using the same bandwidth. The central frequency of each filter is computed depending on the transducer bandwidth. From the probe band-pass defined by $[f_{min}; f_{max}]$, the bandwidth of each filter Δf and the central position of the i^{th} frequency f_i is defined as:

$$\Delta f = (f_{max} - f_{min}) / N \tag{7}$$

$$f_i = f_{min} + (i - 1/2)\Delta f \tag{8}$$

An illustration of the filter family is proposed on Fig. 1.

2.4. Evaluation of the method

The multi-frequency approach was evaluated computing the new resolution and the signal-to-noise ratio (SNR). To evaluate the resolution of the US image, the cross-correlation proposed by Wagner *et al.* has been used [8] to estimate the full width at half maximum in the axial and lateral directions. Moreover, the SNR has been evaluated using:

$$SNR = \mu/\sigma \tag{9}$$

where μ is the mean value of the image and σ is the standard deviation [8]. The SNR is only computed in a region of interest (ROI) depending on the image.

3. RESULTS

3.1. Materials and method

An ideal transducer has been used in simulation, whose characteristics are close to published cMUT measurements [7]. Its frequency characteristic is displayed in Fig. 1. The -6 dB transducer bandwidth is $[1.7; 8.4]$ MHz. These values are used to define the sub-band decomposition.

Two different simulations have been conducted with CREANUIS [9] in order to use the entire bandwidth of the transducer. First a pulse and second a chirp have been transmitted in the medium. The two signals are convolved with the bandwidth. However, the chirp signal has to be correctly designed to fit the bandwidth. The used chirp frequencies bandwidth was the one of the US probe and the transmitted signal was 1 μs long. With such excitation, all the available frequencies are transmitted. With the chirp excitation signal, a compression signal is used in reception to recover the initial axial resolution of the image [10].

The cyst medium has been used in simulation and 100 000 scatterers have been used, randomly set in the medium [11]. Four different areas can be distinguished (Fig. 3): five punctual scatterers on the left, five hyper-echoic cysts in the middle (with increasing diameters versus depth), five hypo-echoic cysts on the right (with decreasing diameters versus depth) and the background. An attenuation of 0.5 dB/cm/MHz has been set in the simulation.

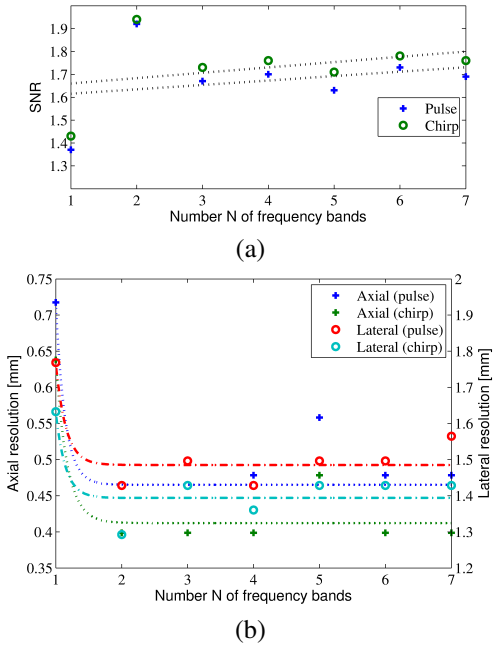

Fig. 2. Estimation of (a) the SNR and (b) the resolutions (axial and lateral) versus the number N of frequency bands for a pulse or a chirp transmitted signals.

3.2. Simulation results

The MF image has been created for different values of N. A maximum value of 7 images has been chosen. In function of the number of images, the frequencies of the frequency bands are updated as in equation (7-8).

For each resulting MF image, the SNR and the resolutions are evaluated and displayed in Fig. 2. The resulting SNR increases with the number of frequency components used in the MF approach. Concerning the resolution, with the increasing number of frequency components, the axial and the lateral resolutions are improved. However, we can appreciate that when pulses are transmitted, a plateau is reached for both lateral and axial resolutions. The corresponding B-mode and MF images are displayed in Fig. 3 in pulse or chirp case. For the B-mode images without compounding, the attenuation compensation has been applied at the central frequency. In the proposed MF images, the resolution is improved at the different depths and for the different cysts. Moreover, the echo intensity is better in the far field, thanks to the attenuation compensation at each specific frequency.

3.3. Experimental results

The experimental evaluation has been carried out using a PZT probe connected to the research scanner Ula-Op [12]. The probe LA523 (Esaote, Firenze) has a -6 dB bandwidth in the range $[4; 10]$ MHz and a 1 μs chirp is used in transmission. A phantom Model 551 (ATS Laboratories, Bridgeport, USA) was used. The manufacturer of the phantom provides an attenuation of 0.5 dB/cm/MHz. Then, the same method has been applied on the receive RF image in order to create the MF image.

The resulting evolution of the SNR and the resolution are displayed in Fig. 4. Both the SNR and the resolution (axial and lateral) are improved when MF scheme is applied. The corresponding B-mode images of the phantom are displayed in Fig. 5. The image on right shows only slight improvements in the contrast while both the axial and lateral resolution seems similar. Visually, the speckle is thinner in the MF image as the resolution around the various wires. On the classical FC image, the obtained SNR is 3.7 with an axial and lateral resolution of 0.69 mm and 0.99 mm, respectively, which demonstrate the increase of SNR and the decrease of resolution compare to classical and MF approach. In MF image, the resolution improvement is reached with a few sub-bands, due to the limited size of the PZT bandwidths. These results confirmed the simulations. The limited improvement of the SNR and resolution may come from the limited depth-of-field used in experimental images.

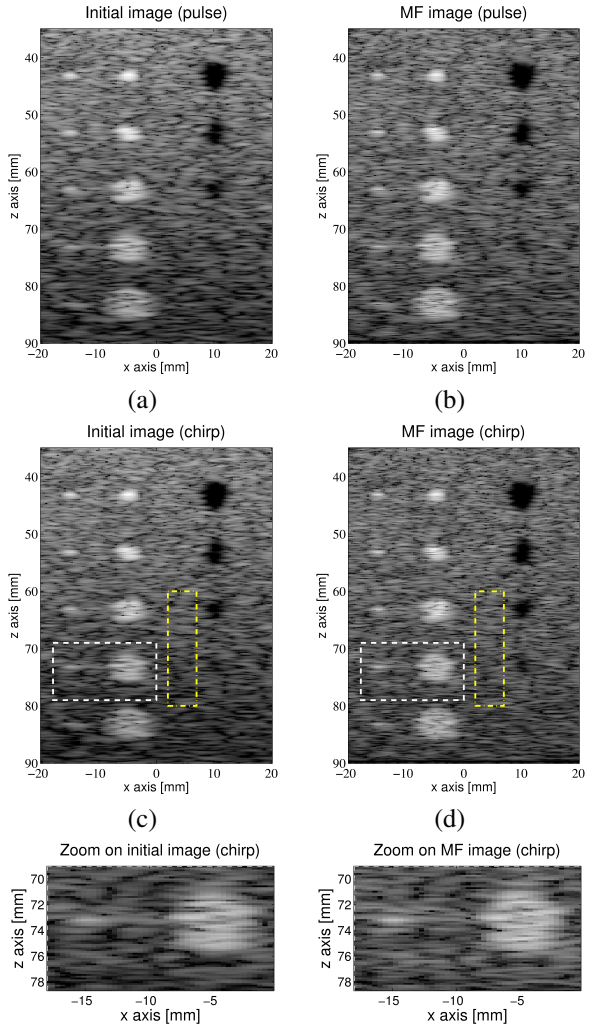

Fig. 3. Resulting B-mode images using pulses (a-b) or chirps (c-d). The left column corresponds to images without compounding and on the right with the MF strategy. White-dashed boxes show the zoomed region of chirp images (e-f) and yellow-dashed-dot boxes display the region where the SNR and the resolution are evaluated.

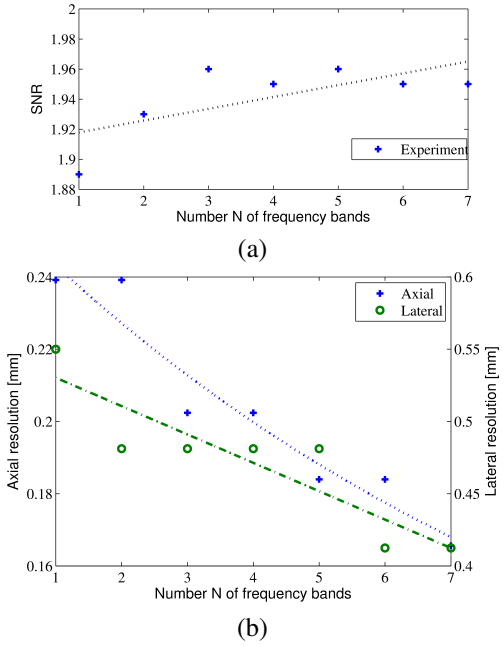

Fig. 4. Estimation of the SNR (a) and the resolution (b) in experimental case.

4. DISCUSSION AND CONCLUSION

This study demonstrated through simulations and experiments that a multi-frequency approach improves both lateral and axial resolutions. Using this strategy, the attenuation compensation provides an enhancement for the regions where the high frequencies are not present. Such compensation increases the resolution of the images at such depths. The multi-frequency is particularly suitable with large bandwidth transducer. Indeed, the required frequencies can be transmitted and recorded into a single transmission while keeping a high frame rate. The increase of the resolution in the MF image opens new perspectives e.g. in imaging method based on speckle tracking. Indeed, the highest resolution of the image leads to more accurate motion estimation.

In term of filtering strategy, the bandwidth was decomposed into N sub-bands, which could be optimized. Different strategies have to be tested as bands with constant $\Delta f/f$, spatio-temporal filtering, continuous filtering, adaptive filtering... The resolution optimization can also be formulated into an inverse problem where an optimal decomposition of the bandwidth has to be found.

Of course, the proposed method has some limitations. First, the method improves the resolution only if attenuation is present. If not, no improvement is measured. Secondly, if the high frequency wave is too low, the MR method increases the noise of the high frequency component that increases the speckle SNR but not the overall resolution. Third, in both simulations and experiments, the attenuation was known and has been perfectly compensated for. In unknown media, a measure of the attenuation at the different frequencies is first required in order to propose the optimal MF image.

In future work, experimental measurements have to be conducted on cMUT array in order to establish the reachable experimental gain in resolution. Moreover, various attenuating media have to be considered to evaluate the MF approach in more realistic cases and the possible increase of the DOF. New phantoms and clinical media have also to be tested with the MF method in order to quantify its contribution.

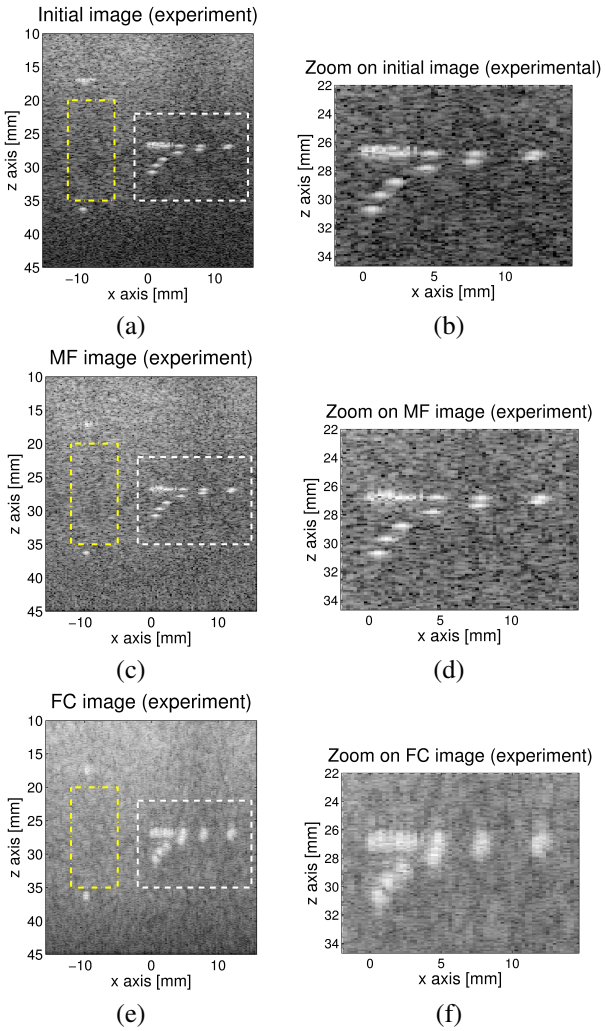

Fig. 5. B-mode image and zoom version of the phantom, (a-b) without compounding and (c-d) after MF strategy and (e-f) with classical FC approach. White-dashed boxes show the zoom region of resulting images and yellow-dash-dot box display the region where the SNR and the resolution are evaluated.

5. ACKNOWLEDGMENTS

The project was partly supported by ANR-07 TecSan-015-01 MONITHER and Centre Lyonnais d'Acoustique (CeLyA), ANR grant n2011-LABX-014.

6. REFERENCES

[1] M. C. van Wijk and J. M. Thijssen, "Performance testing of medical ultrasound equipment: fundamental vs. harmonic mode," *Ultrasonics*, vol. 40, no. 1-8, pp. 585–591, 2002.

[2] D.M. Mills, "Medical imaging with capacitive micromachined ultrasound transducer (cmut) arrays," in *IEEE Ultrasonics Symposium*, 2004, vol. 1, pp. 384–390 Vol.1.

[3] P.A. Magnin, O.T. von Ramm, and F.L. Thurstone, "Frequency compounding for speckle contrast reduction in phased array images," *Ultrasonics Imaging*, vol. 4, no. 3, pp. 267–281, 1982.

[4] I. Claesson and G. Salomonsson, "Frequency- and depth-dependant compensation of ultrasonic signals," *IEEE Transactions on Ultrasonics, Ferroelectrics and Frequency Control*, vol. 35, no. 5, pp. 582–592, 1998.

[5] W.R. Dreschel and K.K. Shung, "Rational attenuation compensation via adaptive digital filtering," in *IEEE Engineering in Medicine and Biology Society*, 1990, pp. 293–294.

[6] Thomas L. Szabo, "Generalized fourier transform diffraction theory for parabolically anisotropic media," *The Journal of the Acoustical Society of America*, vol. 63, no. 1, pp. 28–34, 1978.

[7] A. Novell, M. Legros, N. Felix, and A. Bouakaz, "Exploitation of capacitive micromachined transducers for nonlinear ultrasound imaging," *IEEE Transactions on Ultrasonics, Ferroelectrics and Frequency Control*, vol. 56, no. 12, pp. 2733 –2743, 2009.

[8] R.F. Wagner, S.W. Smith, J.M. Sandrik, and H. Lopez, "Statistics of speckle in ultrasound b-scans," *IEEE Transactions on Sonics and Ultrasonics*, vol. 30, no. 3, pp. 156–163, may 1983.

[9] F. Varray, C. Cachard, P. Tortoli, and O. Basset, "Nonlinear radio frequency image simulation for harmonic imaging: Creanuis," in *IEEE Ultrasonics Symposium*, 2010, pp. 2179–2182.

[10] R.Y. Chiao and X. Hao, "Coded excitation for diagnostic ultrasound: a system developer's perseptive," *IEEE Transactions on Ultrasonics, Ferroelectrics and Frequency Control*, vol. 52, no. 2, pp. 160–170, 2005.

[11] J. A. Jensen and P. Munk, "Computer phantoms for simulating ultrasound b-mode and cfm images," in *23rd Acoustical Imaging Symposium*, 1997.

[12] P. Tortoli, L. Bassi, E. Boni, A. Dallai, F. Guidi, and S. Ricci, "Ula-op: an advanced open platform for ultrasound research," *IEEE Transactions on Ultrasonics, Ferroelectrics and Frequency Control*, vol. 56, no. 10, pp. 2207–2216, 2009.